



1           **Contrasting decadal trends of subsurface excess nitrate in the**  
2           **western and eastern North Atlantic Ocean**

3  
4           Jin-Yu Terence Yang<sup>1,2</sup>, Kitack Lee<sup>1\*</sup>, Jia-Zhong Zhang<sup>3</sup>, Ji-Young Moon<sup>1</sup>,

5                           Joon-Soo Lee<sup>4</sup>, In-Seong Han<sup>4</sup>, and Eunil Lee<sup>5</sup>

6

7       <sup>1</sup> Division of Environmental Sciences and Engineering, Pohang University of Science and  
8       Technology, Pohang 37673, Korea.

9

10       <sup>2</sup> State Key Laboratory of Marine Environmental Science, College of Ocean and Earth Sciences,  
11       Xiamen University, Xiamen 361102, China.

12

13       <sup>3</sup> National Oceanic and Atmospheric Administration, Atlantic Oceanographic and Meteorological  
14       Laboratory, Miami, FL 33149, USA.

15

16       <sup>4</sup> Ocean Climate and Ecology Research Division, National Institute of Fisheries Science, Busan  
17       46083, Korea.

18

19       <sup>5</sup> Ocean Research Division, Korea Hydrographic and Oceanographic Agency, Busan 49111,  
20       Korea.

21

22

23       **\*Corresponding author,**

24       Kitack Lee, Professor

25       Division of Environmental Sciences and Engineering

26       Pohang University of Science and Technology

27       Phone: +82-54-2792285; fax: +82-54-2798299; e-mail: [ktl@postech.ac.kr](mailto:ktl@postech.ac.kr)

28       **Email for other co-authors :**

29       Jin-Yu Terence Yang ([jyyang@xmu.edu.cn](mailto:jyyang@xmu.edu.cn)); Jia-Zhong Zhang ([jia-zhong.zhang@noaa.gov](mailto:jia-zhong.zhang@noaa.gov)); Ji-

30       Young Moon ([todaud@postech.ac.kr](mailto:todaud@postech.ac.kr)); Joon-Soo Lee ([leejoonsoo@korea.kr](mailto:leejoonsoo@korea.kr)); In-Seong Han

31       ([hisjamstec@korea.kr](mailto:hisjamstec@korea.kr)); Eunil Lee ([elee@korea.kr](mailto:elee@korea.kr))

32

33       **Keywords,**

34       anthropogenic nitrogen; excess nitrate; North Atlantic Ocean; climate variability; decadal trend



35 **Abstract**

36 Temporal variations in excess nitrate ( $\text{DIN}_{\text{xs}}$ ) relative to phosphate were evaluated using  
37 datasets derived from repeated measurements along meridional and zonal transects in the upper  
38 (200–600 m) North Atlantic (NAtl) between the 1980s and 2010s. The analysis revealed that the  
39  $\text{DIN}_{\text{xs}}$  trend in the western NAtl differed from that in the eastern NAtl. In the western NAtl,  
40 which has been subject to atmospheric nitrogen deposition (AND) from the USA, the subsurface  
41  $\text{DIN}_{\text{xs}}$  concentrations have increased over the last two decades. This increase was associated with  
42 the increase in AND measured along the US east coast, with a mean lag period of 15 years. This  
43 time lag was approximately equivalent to the time elapsed since the subsurface waters in the  
44 western NAtl were last in contact with the atmosphere (the ventilation age). Our finding provides  
45 an evidence that the  $\text{DIN}_{\text{xs}}$  dynamics in the western NAtl in recent years has been affected by  
46 anthropogenic nitrogen inputs, although this influence is weak relative to that in the North  
47 Pacific. In contrast, a decreasing trend in subsurface  $\text{DIN}_{\text{xs}}$  was observed after the 2000s in the  
48 eastern NAtl, particularly in the high latitudes. This finding may be associated with a possible  
49 decline of tropical  $\text{N}_2$  fixation and the weakening of the Atlantic meridional overturning  
50 circulation, although more time-resolved data on nutrients and meridional circulation are needed  
51 to assess this hypothesis. Our results highlight the importance of both anthropogenic and climate  
52 forcing in impacting the nutrient dynamics in the upper NAtl.

53



## 54 **1. Introduction**

55       The supply of reactive inorganic nitrogen ( $N_r = NO_y + NH_x$ ) to the surface ocean is limited  
56 in most of the oligotrophic marine environments (Fanning, 1989; Moore et al., 2013; Moore,  
57 2016). The addition of  $N_r$  will lead to an increase in primary and export production, and  
58 eventually an enhancement of carbon sequestration in the ocean interior (Okin et al., 2011;  
59 Jickells and Moore, 2015). Anthropogenic nitrogen deposition (AND) to the contemporary ocean  
60 is comparable in magnitude to marine biological  $N_2$  fixation, which has been thought to be the  
61 major external source of  $N_r$  to the oligotrophic ocean (Duce et al., 2008; Fowler et al., 2013;  
62 Jickells et al., 2017). In particular, AND has been found to enhance phytoplankton productivity  
63 in  $N_r$ -depleted tropical and subtropical oceans located downwind of continents that are sources  
64 of pollutant nitrogen (Kim et al., 2014b; St-Laurent et al., 2017). Any changes in this external  
65 source of  $N_r$  induced largely by human activities could cause a wide range of ecological and  
66 biogeochemical consequences (e.g., Doney et al., 2007; Yang et al., 2016).

67       The impact of AND on the dissolved inorganic nitrogen concentration (DIN) in seawater  
68 has recently been assessed in coastal and marginal seas (Kim et al., 2011; Moon et al., 2016), and  
69 in the remote open ocean (Kim et al., 2014a), using historical nutrient concentration datasets.  
70 The analysis of 30 years of data showed that the DIN has increased in marginal seas off the  
71 northeast Asian continent, whereas the dissolved inorganic phosphorus concentration (DIP) has  
72 remained relatively unchanged over this time period (Kim et al., 2011). For open-ocean areas,  
73 the temporal change in excess nitrate relative to DIP ( $DIN_{xs} = DIN - R_{N:P} \times DIP$ , where  $R_{N:P}$  is  
74 the average DIN:DIP ratio of 15:1 for deep waters) was estimated using the relationship between  
75  $DIN_{xs}$  in a particular water parcel and the chlorofluorocarbon (CFC)-12-derived ventilation age  
76 of that parcel (Kim et al., 2014a). An underlying assumption in this analysis is that ocean



77 biological processes (i.e., production and microbial oxidation of organic matter) operate at a  
78 DIN:DIP ratio of 15:1 and thus do not change  $\text{DIN}_{\text{xs}}$ . Changes in seawater  $\text{DIN}_{\text{xs}}$  only occur  
79 when either N input (i.e., AND and  $\text{N}_2$  fixation) or N loss (i.e., denitrification) occurs. The  
80 analysis using this method revealed that the  $\text{DIN}_{\text{xs}}$  has increased in the western North Pacific  
81 Ocean (NPO) since the 1970s (Kim et al., 2014a).

82 The addition of  $\text{N}_r$  to the North Atlantic Ocean (NAtl), which is located downwind from  
83 North America, has more than doubled since 1986 (Galloway et al., 1996). The increasing  
84 addition of  $\text{N}_r$  may lead to an increase in  $\text{DIN}_{\text{xs}}$  in the NAtl (Zamora et al., 2010). However, it  
85 has been argued that  $\text{N}_2$  fixation is a more likely cause of the higher subsurface  $\text{DIN}_{\text{xs}}$  in the  
86 NAtl (Gruber and Sarmiento, 1997; Bates and Hansell, 2004). Differentiating the contributions  
87 of  $\text{N}_2$  fixation and AND is not straightforward because both processes leave similar  
88 biogeochemical signals in seawater, including a high DIN:DIP ratio and low nitrogen isotope  
89 composition (Hastings et al., 2003; Knapp et al., 2010; Yang et al., 2014). In addition to these  
90 two processes, climate variations (commonly expressed as the North Atlantic Oscillation Index)  
91 can concurrently influence the nutrient dynamics in the NAtl (Bates and Hansell, 2004; Singh et  
92 al., 2013). As a result, the processes causing the change in the subsurface  $\text{DIN}_{\text{xs}}$  signal in the  
93 NAtl remain unresolved. This knowledge gap needs to be filled to improve understanding of the  
94 marine nitrogen cycle (Gruber, 2008).

95 The present study was designed to explore the occurrence and rate of decadal change in  
96  $\text{DIN}_{\text{xs}}$  ( $\Delta\text{DIN}_{\text{xs}}$  in  $\mu\text{mol kg}^{-1} \text{decade}^{-1}$ ) in the subsurface NAtl, as well as the explanations for  
97  $\Delta\text{DIN}_{\text{xs}}$ , based on repeat measurements of nutrients and other oceanographic parameters made  
98 over the past three decades or longer.

99



## 100 **2. Materials and methods**

### 101 **2.1. Data**

102 Historical data on temperature, salinity, and the concentrations of nitrate, nitrite, phosphate  
103 and oxygen used in this study have been collected as parts of the Transient Tracers in the Ocean  
104 (TTO), the World Ocean Circulation Experiment (WOCE), the Climate Variability CO<sub>2</sub> Repeat  
105 Hydrography (CLIVAR), and the Global Ocean Ship-Based Hydrographic Investigations (GO-  
106 SHIP) programs. Analysis of nutrient data was based only on concentrations greater than 0.1  
107  $\mu\text{mol kg}^{-1}$  for DIN and 0.01  $\mu\text{mol kg}^{-1}$  for DIP. These concentration levels approximate the  
108 detection limits of DIN and DIP for the analytical methods used in the field observations (Zhang  
109 et al., 2001; Hydes et al., 2010). The data used in our analysis are available at  
110 <https://www.nodc.noaa.gov/ocads/oceans/> (the Global Ocean Data Analysis Project Version 2,  
111 GLODAPv2 product and CLIVAR database).

112 Data analysis was primarily focused on three meridional (A22, A20, and A16N) transects  
113 in the NATl (Fig. 1). A zonal transect (A05) was also included for comparison. All four transects  
114 used in the study are located downwind of the North American continent, which is a major  
115 source region of anthropogenic nitrogen (Fig. 1). Each of these transects was sampled 3 or 4  
116 times during the past 30 years (Table S1). To extend temporal data coverage in the analysis,  
117 historical data obtained from locations adjacent to the four study transects were included in the  
118 analysis. Moreover, the repeat measurements along transect A22 occurred on slightly different  
119 tracks, particularly in the Caribbean Sea and in the northern end of the transect. We therefore  
120 excluded data for areas south of Puerto Rico ( $\sim 18.5^\circ\text{N}$ ) and north of  $36^\circ\text{N}$ , where the distance  
121 between the location of repeat measurements exceeded  $2^\circ$  longitude. Data obtained south of  
122  $20^\circ\text{N}$  along A16N and south of  $15^\circ\text{N}$  along A20 were also excluded from the analysis, because



123 these regions are considerably influenced by the water masses originated from the equatorial  
124 upwelling region (Hansell et al., 2004), and any change in the intensity of upwelling could bias  
125 our analysis of changes in  $\text{DIN}_{\text{xs}}$ . To make datasets collected in different years consistent, an  
126 inverse analysis of repeated measurements made at the same locations was performed to estimate  
127 measurement biases. Any biases found were accounted for by applying adjustment factors to the  
128 original datasets. The adjusted datasets were reported in the GLODAPv2 product and CLIVAR  
129 database (Key et al., 2015; Olsen et al., 2016).

130 The datasets from the GLODAPv2 and CLIVAR did not have systematic biases (Table  
131 S1). To account for any small discrepancies that may exist among the various datasets collected  
132 on the 4 transects, we adjusted the DIN and DIP concentrations based on the assumption that the  
133 physical and chemical properties in deep waters of the tropical and subtropical NATl (south of  
134  $50^{\circ}\text{N}$ ) did not change on decadal time scales (Figs. S1 and S2; see details in Text S1). The mean  
135 corrections were found to be  $0.04 \pm 0.03 \mu\text{mol kg}^{-1}$  for DIN and  $0.006 \pm 0.004 \mu\text{mol kg}^{-1}$  for  
136 DIP, corresponding to their adjustment factors mostly less than 1.5% (Table S2 and Fig. S3).  
137 These corrections fell within the detection limits for DIN and DIP, and were an order of  
138 magnitude smaller than the subsurface  $\Delta\text{DIN}_{\text{xs}}$  signals (see section 3.1). The finding that the  
139 subsurface  $\Delta\text{DIN}_{\text{xs}}$  signals were considerably greater than the detection limit of DIN is a strong  
140 indication that our data adjustments probably did not influence the temporal trend of  $\text{DIN}_{\text{xs}}$ . It  
141 also suggests that our method can extract the decadal trends of  $\text{DIN}_{\text{xs}}$  from less time-resolved  
142 datasets, as has successfully been used in previous studies (Zhang et al., 2000; Ríos et al., 2015;  
143 Woosley et al., 2016).

## 144 **2.2. Relative abundance of DIN over DIP ( $\text{DIN}_{\text{xs}}$ ) in water parcels**



145 We calculated the DIN surplus or deficit relative to DIP in each seawater sample (i.e. the  
146 deviation of the DIN:DIP ratio from that in deep water) by calculating  $DIN_{xs}$  (Fig. 2). This  
147 calculation was performed in the upper 1500 m; and the  $\Delta DIN_{xs}$  signals between GO-SHIP and  
148 WOCE time periods were also evaluated using data obtained from the subsurface layer (200–600  
149 m) because the majority of  $DIN_{xs}$  signals derive from this layer and hence any changes would be  
150 expected to be more marked (see the next section and the  $\Delta DIN_{xs}$  signals at 1200–1500 m for  
151 reference in Fig. 2). In addition, the effect of seasonal variations on  $DIN_{xs}$  signals at this depth  
152 layer is generally insignificant, because seasonal variations are largely confined to waters  
153 shallower than the climatological winter mixed layer (down to 200 m depth). Based on analysis  
154 of data obtained from the BATS site, seasonal variations in subsurface (the target water depth  
155 range) mean  $DIN_{xs}$  values were  $< 0.1 \mu\text{mol kg}^{-1}$  (Note that nutrient data at BATS are available at  
156 [http://batsftp.bios.edu/BATS/bottle/bats\\_bottle.txt](http://batsftp.bios.edu/BATS/bottle/bats_bottle.txt)).

157 The values for  $\Delta DIN_{xs}$  and nutrients in the water column could be biased because of  
158 mixing of water masses having different  $DIN_{xs}$  concentrations, and different nitrogen to  
159 phosphorus ratios associated with organic matter oxidation during various observation periods.  
160 To minimize biases caused by these natural processes, we examined changes in potential  
161 temperature  $\theta$ , salinity and AOU along the potential density surfaces  $\sigma_\theta$  (corresponding to 200–  
162 600 m where the  $DIN_{xs}$  signals are the largest) at  $5^\circ$ – $15^\circ$  latitude or longitude intervals  
163 representing average regional variations along each transect. We found that the  $\theta$  and salinity of  
164 a water mass occupying any given density surface did not change between repeat occupations ( $p$   
165  $> 0.05$ , Student's t-test and ANOVA with Games-Howell test), except for slightly lower  $\theta$  and  
166 salinity since 2000s in the subpolar region (north of  $45^\circ\text{N}$ ) along A16N (Figs. S4 and S5). This  
167 finding is a strong indication that biases in  $\Delta DIN_{xs}$  from the mixing of different water masses



168 were negligible in the subtropical regions over the observation periods (approximately 30 years).  
169 In contrast, we found slight differences in  $\Delta\text{AOU}$  among a few of selected reoccupations (not  
170 shown). To remove the contribution of DIN and DIP from oxidation of organic matter,  
171 adjustment of the nutrient concentrations was made by using the DIP:DIN:O<sub>2</sub> remineralization  
172 ratio of 1:15:(-160) derived from data along the  $\sigma_{\theta} = 27.0$  horizon in the NATl (Takahashi et al.,  
173 1985; Anderson and Sarmiento, 1994). The estimated DIN:DIP ratio for remineralization of  
174 organic matter was in the range 15–18 (Takahashi et al., 1985; Anderson and Sarmiento, 1994).  
175 The chosen value of the DIN:DIP ratio for remineralization did not significantly change the  
176 patterns of  $\Delta\text{DIN}_{\text{xs}}$ . Therefore, the  $\Delta\text{DIN}_{\text{xs}}$  within the layer of the  $\text{DIN}_{\text{xs}}$  maxima along all  
177 transects examined were free from biases of either mixing of water masses or changes in  
178 oxidation of organic matter. For each subregion,  $\text{DIN}_{\text{xs}}$  (or DIP) anomalies indicated individual  
179  $\text{DIN}_{\text{xs}}$  (or DIP) values minus the mean  $\text{DIN}_{\text{xs}}$  (or DIP) values from the GO-SHIP dataset (Figs.  
180 3–5). Note that the positive anomalies indicate higher values than the GO-SHIP data.

181

### 182 **3. Results and discussion**

#### 183 **3.1. Decadal variations of $\text{DIN}_{\text{xs}}$ in the upper North Atlantic Ocean**

184 High  $\text{DIN}_{\text{xs}}$  values were broadly distributed in the subsurface waters (< 1000 m) in the  
185 NATl. In particular, the maximum  $\text{DIN}_{\text{xs}}$  values were found between 200 and 600 m (Fig. 2), and  
186 were slightly higher in the western basin (an average value of  $1.4 \pm 0.3 \mu\text{mol kg}^{-1}$  was calculated  
187 for A22 in 2012) than those in the eastern basin (an average value of  $0.8 \pm 0.2 \mu\text{mol kg}^{-1}$  was  
188 calculated for A16N in 2013). Similarly, the west-east gradient in  $\text{DIN}_{\text{xs}}$  was apparent along the  
189 zonal transect A05 at 24.5°N latitude (Fig. S6).





190 Based on multiple cruises along each transect, changes in  $\text{DIN}_{\text{xs}}$  were discernable over the  
191 decadal periods; these changes were most pronounced between 200 m and 600 m (Fig. 2). The  
192 rate of  $\Delta\text{DIN}_{\text{xs}}$  in the NATl differed among locations of transects between GO-SHIP and WOCE  
193 periods. Specifically, the  $\Delta\text{DIN}_{\text{xs}}$  values were mostly positive in the western NATl (A22 and  
194 A20), where they varied from 0.02 to 0.33  $\mu\text{mol kg}^{-1} \text{decade}^{-1}$ , with the highest rate found at  
195 31°N–36°N along A22. In contrast, the  $\Delta\text{DIN}_{\text{xs}}$  values became negative in the eastern NATl  
196 (20°N–60°N along A16N), where they ranged from –0.07 to –0.40  $\mu\text{mol kg}^{-1} \text{decade}^{-1}$ ; the  
197 greatest rate of  $\text{DIN}_{\text{xs}}$  decrease was in the subpolar region (north of 45°N). Moreover, the  $\Delta\text{DIN}_{\text{xs}}$   
198 values remained close to zero in the intermediate waters (1200–1500 m) in the western and  
199 eastern subtropical NATl (Fig. 2). This observation confirms that the marked changes in  $\text{DIN}_{\text{xs}}$   
200 largely occurred in the subsurface waters.

201 The  $\Delta\text{DIN}_{\text{xs}}$  in the NATl showed geographically distinct patterns after removing the  
202 influence of remineralization of organic matter (Fig. 3). We found that the  $\Delta\text{DIN}_{\text{xs}}$  within the  
203 layer of the  $\text{DIN}_{\text{xs}}$  maximum decreased since 1997 (measurement year) along the transects near  
204 the source continent (i.e. the entire transect of A22, and 31°N–36°N along A20) (Figs. 3a and  
205 3b), and its rates ranged from 0.19 to 0.33  $\mu\text{mol kg}^{-1} \text{decade}^{-1}$  (Fig. 2). The trend in  $\text{DIN}_{\text{xs}}$  found  
206 at the BATS site is broadly comparable to that found between 31°N and 36°N along A22 (Fig.  
207 3a). The rate of increase of  $\text{DIN}_{\text{xs}}$  at the BATS site since the late 1990s (0.40  $\mu\text{mol kg}^{-1} \text{decade}^{-1}$ )  
208 was also similar to that observed in the latitude band 31°N–36°N along A22. Such agreement  
209 with time series data strengthens our finding derived from less time-resolved datasets.

210 The discernable increase in  $\text{DIN}_{\text{xs}}$  rapidly diminished in the central gyre of the NATl  
211 (15°N–31°N for A20, 20°N–45°N for A16N and A05), where the  $\Delta\text{DIN}_{\text{xs}}$  was statistically  
212 insignificant ( $p > 0.05$ , Student's t-test and ANOVA with Games-Howell test; Figs. 3 and S7).



213 Furthermore, the level of  $\text{DIN}_{\text{xs}}$  appeared to decrease at high latitudes in the eastern NATl (north  
214 of  $45^{\circ}\text{N}$  on A16N; Fig. 3c). The trend of decrease has been more pronounced since the 2000s in  
215 this region, and occurred concurrently with decreases in temperature and salinity ( $p < 0.05$ ,  
216 Student's t-test and ANOVA with Games-Howell test; Figs. S4c and S5c). Our observations  
217 indicate that the mechanisms responsible for the  $\Delta\text{DIN}_{\text{xs}}$  in the subtropical and subpolar NATl are  
218 likely to differ.

### 219 **3.2 AND influence on the $\Delta\text{DIN}_{\text{xs}}$ in the western North Atlantic Ocean**

220 More pronounced increase in the subsurface  $\text{DIN}_{\text{xs}}$  has been observed in recent decades in  
221 the western mid-latitude NATl (Fig. 3), which is subject to considerable AND input from the  
222 North American continent. Recent studies suggest that the reduced form of nitrogen entering the  
223 NATl is primarily of marine autochthonous origin, rather than of anthropogenic origin (i.e.  
224 atmospheric deposition) (Altieri et al., 2014; Altieri et al., 2016). Thus, this autochthonous  
225 reduced nitrogen would not influence seawater  $\text{DIN}_{\text{xs}}$  values. Therefore, we only included the  
226 effect of  $\text{NO}_x$  emissions and deposition (mostly in the forms of  $\text{NO}_3^-$  and  $\text{HNO}_3$ ; hereinafter  $\text{NO}_x$   
227 is used to represent the major form of AND) on the  $\Delta\text{DIN}_{\text{xs}}$  values (Figs. 1 and 5b). From the  
228 1970s to the 2010s the  $\text{NO}_x$  emissions from the USA showed a three-phase temporal transition  
229 (EPA, 2000). The  $\text{NO}_x$  emissions from the USA increased from 1970 to the mid 1980s, and  
230 stayed at high levels for approximately 20 years, and then decreased gradually after the mid  
231 2000s as a result of the regulation of air pollutant emissions throughout the North American  
232 continent (Fig. 5b). The anthropogenic nitrogen pollutants are mostly transported eastward and  
233 ultimately deposited in the western NATl (Fig. 1).

234 Although there are limited data (time and space) on wet deposition of  $\text{NO}_x$ , the temporal  
235 pattern based on measurements on the US Atlantic coast is comparable to that for the  $\text{NO}_x$



236 emissions. For example, based on data obtained from the National Atmospheric Deposition  
237 Program (NADP; <http://nadp.sws.uiuc.edu/>), there was an increase from the 1980s to early  
238 1990s, and the level remained high for approximately 15 years and then decreased (Fig. 5b). This  
239 trend of wet deposition of NO<sub>x</sub> was commonly found at AND monitoring sites located along the  
240 US Atlantic coast (Table S3).

241 The AND signals can be transported to the subsurface waters of the mesopelagic western  
242 NATl via two associated mechanisms. The first process involves production and bacterial  
243 oxidation of organic matter. In these biological processes, new anthropogenic nitrogen added by  
244 atmospheric deposition are removed from the surface via photosynthetic utilization by  
245 phytoplankton and gravitational sinking of the resulting organic matter with N:P ratio higher  
246 than 15:1 (Singh et al., 2013). These N-rich organic matters are subsequently remineralized by  
247 bacteria at depth (Antia, 2005). This process involving well-known biological processes would  
248 facilitate the transfer of high surface N:P signals to the subsurface waters. The second process  
249 involves the physical transport of surface waters with greater N:P signals, which is a plausible  
250 mechanism for generating the subsurface AND signals observed in the western NATl. High  
251 inputs of NO<sub>x</sub> by atmospheric deposition occur over the coastal areas of the NATl and are mostly  
252 entrained in areas close to the northern edge of the western NATl via the strong and persistent  
253 western boundary current (i.e. the Gulf Stream, Fig. 1). Both active winter mixing and the  
254 concurrent formation of mode water in this region would be expected to facilitate the transport of  
255 surface waters loaded with high DIN<sub>xs</sub> (and anthropogenic CO<sub>2</sub> and CFCs) to the subsurface  
256 layer, and to spread these DIN<sub>xs</sub>-loaded waters southward (Palter et al., 2005).

257 The substantial increase in subsurface DIN<sub>xs</sub> after 1997 (approximately equal to the pCFC-  
258 12 ventilation year of 1982) at sites having greater inputs of AND (boxes 1–3 in Fig. 5a, and at



259 the BATS site) appears to coincide with the increasing wet deposition of  $\text{NO}_x$  from the US  
260 continent, with a lag period of approximately 15 years. The time lag observed is approximately  
261 equal to the ventilation age of the target subsurface waters in this region, which was estimated to  
262 be 6–25 years based on the CFCs concentrations (Hansell et al., 2004; Hansell et al., 2007). The  
263 time lag suggests that the physical mechanism is important in transporting the AND signals to  
264 the subsurface waters, although the mismatch between the observed time lag and the ventilation  
265 age of water masses may be due, at least in part, to the biological processes.

266 The rates of  $\text{DIN}_{\text{xs}}$  increase ( $0.19\text{--}0.33 \mu\text{mol kg}^{-1} \text{ decade}^{-1}$ ; boxes 1–3 in Fig. 5a) measured  
267 in the western NATl (reported in the preceding section) are equivalent to an increase of 78–135  
268  $\text{mmol N m}^{-2} \text{ decade}^{-1}$  in the subsurface N inventory (200–600 m) of the western NATl. This is  
269 slightly higher than the increase in wet  $\text{NO}_x$  deposition (approximately  $60 \text{ mmol N m}^{-2} \text{ decade}^{-1}$ )  
270 measured along the US east coast from the 1980s to the 2000s (Fig. 5b), but is broadly consistent  
271 with the total  $\text{NO}_x$  fluxes (approximately  $90 \text{ mmol N m}^{-2} \text{ decade}^{-1}$ ) if dry deposition is included  
272 in the modeled and observed results (Dentener et al., 2006; Baker et al., 2010). We thus suggest  
273 that anthropogenic nitrogen input is probably a main driver of  $\text{DIN}_{\text{xs}}$  increase in the western  
274 basin. An anthropogenic influence manifested in oceanic nutrient dynamics having a lag period  
275 of 15 years, has also been detected at 200–600 m in the Mediterranean Sea, where Moon et al.,  
276 (2016) showed a three-phase temporal transition (a trend of increase–stability–decline) in DIN  
277 concentration between 1985 and 2014; this was probably associated with corresponding changes  
278 in anthropogenic nitrogen input.

279 The temporal trend of the nitrogen isotope record ( $\text{CS-}\delta^{15}\text{N}$ ) measured on the Bermuda  
280 coral skeleton is comparable to the trends of  $\text{NO}_x$  emission from the USA (Fig. S8), indicating  
281 that the AND signals have been embedded in the coral  $\delta^{15}\text{N}$  record. The  $\text{CS-}\delta^{15}\text{N}$  record on the



282 Bermuda coral reflects the annual biological response to the local AND signals in the surface  
283 waters; hence, its trend may follow changes in anthropogenic  $\text{NO}_x$  input without a time lag. For  
284 the western NATl, the rates of  $\text{DIN}_{\text{xs}}$  increase we found are in agreement with those from the  
285 earlier studies using different datasets and methodologies (Hansell et al., 2007; Landolfi et al.,  
286 2008; Singh et al., 2013), but are lower than those observed in the NPO ( $0.30\text{--}1.20 \mu\text{mol kg}^{-1}$   
287  $\text{decade}^{-1}$ , Kim et al., 2014a). The different rates of seawater  $\text{DIN}_{\text{xs}}$  increase found between the  
288 western NATl and NPO appear to be consistent with the  $\text{CS-}\delta^{15}\text{N}$  records in these two basins.  
289 During the 20<sup>th</sup> century, a small decline ( $-0.2\text{‰}$ ) in  $\text{CS-}\delta^{15}\text{N}$  was observed in corals from  
290 Bermuda (Wang et al., 2018), whereas a greater decrease ( $-0.7\text{‰}$ ) in  $\text{CS-}\delta^{15}\text{N}$  was detected from  
291 the South China Sea (Ren et al., 2017). The lower rates of seawater  $\text{DIN}_{\text{xs}}$  increase (or slower  
292 decline in  $\text{CS-}\delta^{15}\text{N}$ ) in the NATl were likely due to the lower rate of nitrogen emissions (also  
293 indicating nitrogen deposition) from the North American continent ( $0.15 \text{ Tg N year}^{-1}$  observed  
294 from 1970 to 2000; EPA, 2000) than from northeast Asia ( $0.40 \text{ Tg N year}^{-1}$  observed from 1980  
295 to 2010; Liu et al., 2013). In this case, the recent trend of decreasing emission in anthropogenic  
296 nitrogen from North America, as well as the decrease in wet nitrogen deposition observed along  
297 the US east coast, may reverse the pattern of the increase in subsurface  $\text{DIN}_{\text{xs}}$  in the western  
298 NATl in the near future. Indeed, this reversed pattern appears to have emerged recently at the  
299 BATS site (Figs. 3a and 5b), based on more time-resolved observations. Together, our findings  
300 suggest that the AND has affected the nutrient dynamics in the western NATl, although the  
301 magnitude of this effect is relatively small, and its influence would be expected to become less  
302 significant under a scenario of increased control of pollutant emissions.

### 303 **3.3. Biogeochemical processes that may affect the $\Delta\text{DIN}_{\text{xs}}$ in the western North Atlantic**

#### 304 **Ocean**



305 Other biogeochemical processes may also affect the observed pattern of  $\Delta\text{DIN}_{\text{xs}}$  in the  
306 western NATl. Nitrogen fixation contributes considerably to the total export production ( $1.3\text{--}3.8$   
307  $\text{mol C m}^{-2} \text{ year}^{-1}$ ; Lee, 2001) in oligotrophic gyres of the NATl (Lee et al., 2002; Ko et al., 2018),  
308 which could therefore generate the positive signals of  $\text{DIN}_{\text{xs}}$  in subsurface waters (Hansell et al.,  
309 2004). The rate of  $\text{N}_2$  fixation and the abundance of diazotrophs have been reported to be highest  
310 (Luo et al., 2012; Benavides and Voss, 2015) in the subtropical gyre of the western NATl (see  
311 boxes 4–6 in Fig. 5a), however, the subsurface  $\text{DIN}_{\text{xs}}$  did not change significantly among the  
312 repeat occupations of transects (Figs. 3 and S7a). No direct evidence for increasing activity of  
313 diazotrophs in the NATl is available (Mahaffey et al., 2005; Benavides and Voss, 2015). Contrary  
314 to our expectation, the increase in subsurface  $\text{DIN}_{\text{xs}}$  was only found upstream of the subduction  
315 zone (north of the hot spots for  $\text{N}_2$  fixation; Figs. 3 and 5a). In this region (boxes 1–3) the  
316 observed rate of  $\text{N}_2$  fixation was  $4.2 \text{ mmol m}^{-2} \text{ year}^{-1}$  (Luo et al., 2012), considerably lower than  
317 the atmospheric  $\text{NO}_x$  deposition ( $10\text{--}40 \text{ mmol m}^{-2} \text{ year}^{-1}$ ; see Fig. 1). If  $\text{N}_2$  fixation mainly  
318 drives the increase in subsurface  $\text{DIN}_{\text{xs}}$  in this region, its rate would have been expected to  
319 increase by 2 to 3-fold during recent decades. Such an increase in  $\text{N}_2$  fixation activity is highly  
320 unlikely (Benavides and Voss, 2015). Moreover, if  $\text{N}_2$  fixation activity had increased during the  
321 study period we would expect the DIP concentration decreases in the surface ocean and  
322 concurrently increases below (Kim et al., 2014a), but this was not observed (Fig. 4). Therefore,  
323  $\text{N}_2$  fixation has probably not been a major factor leading to the increase in  $\text{DIN}_{\text{xs}}$  in the western  
324 NATl over the study period.

325 Remineralization of particulate and dissolved organic matters (POM and DOM) is another  
326 potential source of subsurface  $\text{DIN}_{\text{xs}}$  in the NATl, as a result of the high N:P ratios of organic  
327 matters and the preferential remineralization of P from POM and DOM (Landolfi et al., 2008;



328 Lomas et al., 2010). The DON concentration in the subsurface waters in the western NATl (near  
329 the BATS site), however, remained unchanged during the period 1998–2011 ([http://bats.bios.  
330 edu/](http://bats.bios.edu/)). Moreover, the N:P ratios in DOM and suspended POM obtained at 0–100 m at the BATS  
331 site did not change between 2004 and 2012 (Singh et al., 2015). Likewise, we did not find any  
332 discernible interannual changes in the N:P ratio of sinking particles collected between 150 and  
333 300 m at the BATS site (Fig. S9). Thus, the change in subsurface  $\text{DIN}_{\text{xs}}$  in the western NATl was  
334 not primarily driven by variable N:P ratios of sinking POM. Taken together, these findings  
335 suggest that DOM and POM remineralization has not contributed to the  $\Delta\text{DIN}_{\text{xs}}$  in the subsurface  
336 waters of the western NATl during the periods in this study. Having excluded  $\text{N}_2$  fixation and  
337 remineralization of organic matters as key drivers, we hypothesize that the addition of AND has  
338 been the major contributor to the recent increases in subsurface  $\text{DIN}_{\text{xs}}$  in the western NATl.

### 339 **3.4. Influences of climate variability on the $\Delta\text{DIN}_{\text{xs}}$ in the western North Atlantic Ocean**

340 As a prevailing climate mode over the NATl, the North Atlantic Oscillation (NAO) strongly  
341 influences the formation of the subtropical mode water (STMW) in the western NATl, which in  
342 turn affects subsurface nutrient and  $\text{DIN}_{\text{xs}}$  concentrations in the downstream region (Bates and  
343 Hansell, 2004; Palter et al., 2005). The STMW is known to form in areas south of the Gulf  
344 Stream extension, and then primarily flows southward to the entire western basin; its intrusion to  
345 the eastern basin has been suggested to be minor (Palter et al., 2005; Palter et al., 2011). The  
346 formation of the STMW is generally enhanced when the NAO index becomes negative. During  
347 this negative phase of the NAO, an increased contribution of low-nutrient water to the STMW  
348 lowers the subsurface nutrient concentrations and  $\text{DIN}_{\text{xs}}$  in the subtropical gyre. In contrast,  
349 during the positive phase of the NAO, the STMW formation becomes weaker, and thus the  
350 subsurface nutrient concentrations and  $\text{DIN}_{\text{xs}}$  would increase downstream of the STMW



351 formation region (Palter et al., 2005). The winter (December–March) NAO index has been  
352 mostly positive values since 1980, although its trend appeared to show an increase before the  
353 early 1990s and to decrease slightly thereafter (Fig. S10). Contrary to the trend in this  
354 atmospheric forcing, our nutrient data showed no evident changes in the subsurface DIP in the  
355 downstream region (e.g. A22 and A20;  $p > 0.05$ , Student's t-test and ANOVA with Games-  
356 Howell test; Figs. 4 and S7b) over the past 3 decades, irrespective of changes in the NAO index.  
357 These observations indicate that the basin-wide  $\Delta\text{DIN}_{\text{xs}}$  are probably less likely controlled by a  
358 persistent positive phase of the NAO. Time-series data further strengthened the conclusion  
359 drawn from the basin-scale data. For example, the decline in the Bermuda CS- $\delta^{15}\text{N}$  value was  
360 accompanied by several superimposed decadal oscillations induced by the NAO (Wang et al.,  
361 2018). Similarly, such oscillations appear to be imprinted in the time-series measurements of  
362 subsurface  $\text{DIN}_{\text{xs}}$  at the BATS site (Fig. 5b). Nonetheless, the basin-wide  $\Delta\text{DIN}_{\text{xs}}$  trends induced  
363 by anthropogenic inputs of nitrogen are still visible.

### 364 **3.5. Subsurface $\Delta\text{DIN}_{\text{xs}}$ trend in the eastern North Atlantic Ocean**

365 There was an apparent decrease in subsurface  $\text{DIN}_{\text{xs}}$  in the eastern NATl (e.g. A16N),  
366 which is the opposite trend to that found in the western NATl (Fig. 5a). The decreasing trend ( $-$   
367  $0.40 \mu\text{mol kg}^{-1} \text{decade}^{-1}$ ) in the subsurface  $\text{DIN}_{\text{xs}}$  in the eastern subpolar NATl ( $45^\circ\text{N}$ – $60^\circ\text{N}$   
368 along A16N) has been more evident since the 2000s (Fig. 3c). A similar decrease in the  
369 subsurface (300–500 m) DIN between 1998 and 2013 was also found at a site ( $68.0^\circ\text{N}$ ,  $12.7^\circ\text{W}$ )  
370 in the northern Iceland Sea, but little change in DIP was observed (Fig. S12). The  
371 remineralization of DOM may play an important role (Kähler et al., 2010); however, due to  
372 insufficient time-resolved data, we could not confirm whether there was any decrease in the rate  
373 of DOM remineralization in the eastern subpolar NATl. From 1999 to 2009,  $\text{NO}_x$  emission from





374 Europe has decreased by 31%, mainly owing to change in energy consumption from fossil fuels  
375 to nuclear power (Vet et al., 2014). This decline in recent  $\text{NO}_x$  emission from Europe (the blue  
376 solid line in Fig. S11) is a viable explanation for the decrease in subsurface  $\text{DIN}_{\text{xs}}$  in the eastern  
377 subtropics. However, much of the  $\text{NO}_x$  derived from Europe is probably deposited to the  
378 European coasts, because the prevailing westerly winds carry it eastward to the eastern European  
379 continent (Fig. 1) (Baker et al., 2010). Moreover, the amounts of  $\text{NO}_x$  deposited onto the eastern  
380 subpolar basin ( $< 10 \text{ mmol N m}^{-2} \text{ year}^{-1}$ ) were found to be small (Fig. 1). In the extreme scenario  
381 in which no such  $\text{NO}_x$  deposition occurred during the period of analysis, the lack of this  $\text{NO}_x$   
382 deposition would only account for  $< 20\%$  of the total decline in subsurface  $\text{DIN}_{\text{xs}}$  in the eastern  
383 subpolar NATl (Fig. 2c). This suggests that the influence of European AND on seawater nutrient  
384 dynamics in the eastern subtropical NATl is minimal (Hansell et al., 2007).

385       A recent study reported that most  $\text{N}_2$  fixation occurs in the tropical NATl (south of  $24^\circ\text{N}$ ;  
386 Marconi et al., 2017). The upper loop of the Atlantic meridional overturning circulation (AMOC)  
387 acts as a passage through which nutrients are transported from the tropical regions to the  
388 subpolar gyre (Pelegri and Csanady, 1991; Williams et al., 2006; Moore et al., 2009). Therefore,  
389 a decreasing rate of  $\text{N}_2$  fixation is another likely explanation for the decreasing trend in  
390 subsurface  $\text{DIN}_{\text{xs}}$  in the eastern NATl. Indeed, the supply of iron and phosphorus from Africa to  
391 the eastern tropical and subtropical NATl has declined by approximately 10% per decade during  
392 the period 1980–2008 (Foltz and Mcphaden 2008; Ridley et al., 2014), and was likely  
393 accompanied by a reduction in the growth of diazotrophs in the eastern tropical NATl (Mills et  
394 al., 2004; Benavides et al., 2013). On the other hand, the decrease in the subpolar subsurface  
395  $\text{DIN}_{\text{xs}}$  occurred concurrently with decreases in temperature and salinity at the same water depth  
396 in the subpolar region (Figs. 3c, S4c and S5c). These observations of concurrent cooling and



397 freshening were suggested to be associated with the fact that the strength of ocean circulation (as  
398 well as heat transport) in the NATl is decreasing, as a result of weakening of the AMOC since  
399 2005 (Srokosz and Bryden, 2015; Robson et al., 2016). Therefore, the observed weakening in the  
400 northward transport of tropical waters might in part contribute to a reduction in the  $DIN_{xs}$   
401 signature in the subpolar gyres of the eastern NATl, as seen north of  $45^{\circ}N$  on A16N (Fig. 5a).  
402 This result is consistent with a reduction in the subsurface  $DIN_{xs}$  observed in the north Iceland  
403 Sea since 2005 (Fig. S12d). If this mechanism plays a governing role, changes in nutrient  
404 supplies related to a reduction of the AMOC would have a large impact on biological export and  
405 the marine ecosystem (Schmittner, 2005). Although compelling, our observations are not a direct  
406 confirmation that decline in  $N_2$  fixation rate and variations in the AMOC are the main cause of  
407 the decreasing trend in subsurface  $DIN_{xs}$  in the eastern subpolar region. Therefore, this finding  
408 remains a working hypothesis that needs confirmation using more time-resolved data in future  
409 studies.

410

#### 411 **4. Conclusions and implication**

412 Our results support that AND has been a cause of the temporal variations in seawater  
413  $DIN_{xs}$  in the subsurface waters of the western NATl during the recent 3 decades. In the eastern  
414 subtropical NATl, the decline in  $NO_x$  emission from Europe, and possibly a decrease in the  $N_2$   
415 fixation rate, are likely drivers of subsurface  $DIN_{xs}$  change. However, in the subpolar gyres of  
416 the eastern NATl the subsurface  $DIN_{xs}$  has decreased since the 2000s, as a result of a possible  
417 decrease in  $N_2$  fixation. Recent changes in ocean circulation (e.g., the AMOC) might also play a  
418 role. Ocean circulation did not directly influence the  $DIN_{xs}$  in the water column, but it rather  
419 redistributed the  $DIN_{xs}$  over the basin in the NATl. This mechanism requires confirmation based



420 on new data. Our study also shows that both human activities and climate variations together  
421 exert a discernable impact on the decadal variations of  $\text{DIN}_{\text{xs}}$  in the subsurface waters of the  
422 NATl.

423 Human activities may have begun to influence the concentrations and stoichiometry of  
424 nutrients, at least in the western NATl, and profound changes have been verified on the western  
425 NPO (Kim et al., 2014a) and Mediterranean Sea (Moon et al., 2016). These findings indicate  
426 global-scale changes in marine biogeochemistry, caused by human activities that are  
427 simultaneously influencing carbon sequestration and greenhouse gas emission (e.g.,  $\text{N}_2\text{O}$ ) (Duce  
428 et al., 2008). Continuing monitoring of changes in  $\text{DIN}_{\text{xs}}$  in the NATl are needed to determine  
429 whether the levels have followed the recent decrease in AND, particularly in the USA. Such  
430 external perturbations could also alter the close homeostasis of the marine N cycle and its  
431 feedback to climate (Gruber and Deutsch, 2014).



432 **Supporting information**

433 Detailed description of transects used in the analysis, and additional tables and figures.

434

435 **Author contribution**

436 JYTY and KL designed the present work and drafted the manuscript. JYTY and JYM did  
437 the data analysis. JZZ, ISH, JSL, and EL contributed to discussion and interpretation of the data.

438

439 **Competing interests**

440 We have no conflict of interest to declare.



## 441 **Acknowledgements**

442           We wish to thank all of scientists who contributed to data used in this study. This work  
443 was supported by the National Institute of Fisheries Science (R2020044) and by "Management of  
444 Marine Organisms causing Ecological Disturbance and Harmful Effects" funded by the Ministry  
445 of Ocean and Fisheries (MOF). Additional support for JYTY was provided by “The Principal’s  
446 Fund” of Xiamen University (ZK1114). JZZ was supported by NOAA Ocean and Atmospheric  
447 Research. The scientific results and conclusions, as well as any views or opinions expressed  
448 herein, are those of the authors and do not necessarily reflect the views of NOAA or the US  
449 Department of Commerce. This is the State Key Laboratory of Marine Environmental Science  
450 contribution NO. melpublication2020387.



## 451 **References**

- 452 Altieri, K. E., Fawcett, S. E., Peters, A. J., Sigman, D. M., and Hastings, M. G.: Marine biogenic  
453 source of atmospheric organic nitrogen in the subtropical North Atlantic, Proc. Natl. Acad.  
454 Sci., 113, 925-930, <http://doi.org/10.1073/pnas.1516847113>, 2016.
- 455 Altieri, K. E., Hastings, M. G., Peters, A. J., Oleynik, S., and Sigman, D. M.: Isotopic evidence  
456 for a marine ammonium source in rainwater at Bermuda, Global Biogeochem. Cycles, 28,  
457 1066-1080, <http://doi.org/10.1002/2014GB004809>, 2014.
- 458 Anderson, L. A., and Sarmiento, J. L.: Redfield ratios of remineralization determined by nutrient  
459 data analysis, Global Biogeochem. Cycles, 8, 65-80, <http://doi.org/10.1029/93GB03318>,  
460 1994.
- 461 Antia, A. N.: Solubilization of particles in sediment trap, revising the stoichiometry of mixed  
462 layer export, Biogeosciences, 2, 189-204, <http://doi.org/10.5194/bg-2-189-2005>, 2005.
- 463 Baker, A. R., Lesworth, T., Adams, C., Jickells, T. D., and Ganzeveld, L.: Estimation of  
464 atmospheric nutrient inputs to the Atlantic Ocean from 50°N to 50°S based on large-scale  
465 field sampling: Fixed nitrogen and dry deposition of phosphorus, Global Biogeochem. Cycles,  
466 24, GB3006, <http://doi.org/10.1029/2009GB003634>, 2010.
- 467 Bates, N. R., and Hansell, D. A.: Temporal variability of excess nitrate in the subtropical mode  
468 water of the North Atlantic Ocean, Mar. Chem., 84, 225-241,  
469 <http://doi.org/10.1016/j.marchem.2003.08.003>, 2004.
- 470 Benavides, M., and Voss, M.: Five decades of N<sub>2</sub> fixation research in the North Atlantic Ocean,  
471 Front. Mar. Sci., 2, 40, <http://doi.org/10.3389/fmars.2015.00040>, 2015.
- 472 Benavides, M., Arístegui, J., Agawin, N. S. R., Cancio, J. L., and Hernández-León, S.:  
473 Enhancement of nitrogen fixation rates by unicellular diazotrophs vs. *Trichodesmium* after a  
474 dust deposition event in the Canary Islands, Limnol. Oceanogr., 58, 267-275,  
475 <http://doi.org/10.4319/lo.2013.58.1.0267>, 2013.
- 476 Dentener, F., Drevet, J., Lamarque, J. F., Bey, I., Eickhout, B., Fiore, A. M., Hauglustaine, D.,  
477 Horowitz, L. W., Krol, M., Kulshrestha, U. C., Lawrence, M., Galy-Lacaux, C., Rast, S.,  
478 Shindell, D., Stevenson, D., Van Noije, T., Atherton, C., Bell, N., Bergman, D., Butler, T.,  
479 Cofala, J., Collins, B., Doherty, R., Ellingsen, K., Galloway, J., Gauss, M., Montanaro, V.,  
480 Müller, J. F., Pitari, G., Rodriguez, J., Sanderson, M., Solmon, F., Strahan, S., Schultz, M.,  
481 Sudo, K., Szopa, S., and Wild, O.: Nitrogen and sulfur deposition on regional and global



- 482 scales: A multimodel evaluation, *Global Biogeochem. Cycles*, 20, GB4003,  
483 <http://doi.org/10.1029/2005gb002672>, 2006.
- 484 Doney, S. C., Mahowald, N., Lima, I., Feely, R. A., Mackenzie, F. T., Lamarque, J. -F., and  
485 Rasch, P. J.: Impact of anthropogenic atmospheric nitrogen and sulfur deposition on ocean  
486 acidification and the inorganic carbon system, *Proc. Natl. Acad. Sci.*, 104, 14580-14585,  
487 <http://doi.org/10.1073/pnas.0702218104>, 2007.
- 488 Duce, R. A., LaRoche, J., Altieri, K., Arrigo, K. R., Baker, A. R., Capone, D. G., Cornell, S.,  
489 Dentener, F., Galloway, J., Ganeshram, R. S., Geider, R. J., Jickells, T., Kuypers, M. M.,  
490 Langlois, R., Liss, P. S., Liu, S. M., Middelburg, J. J., Moore, C. M., Nickovic, S., Oschlies,  
491 A., Pedersen, T., Prospero, J., Schlitzer, R., Seitzinger, S., Sorensen, L. L., Uematsu, M.,  
492 Ulloa, O., Voss, M., Ward, B., and Zamora, L.: Impacts of atmospheric anthropogenic  
493 nitrogen on the open ocean, *Science*, 320, 893-897, <http://doi.org/10.1126/science.1150369>,  
494 2008
- 495 EPA: National Air Pollutant Emission Trends, 1900–1998, Office of Air Quality Planning and  
496 Standards, Research Triangle Park, 2000.
- 497 Fanning, K. A.: Influence of atmospheric pollution on nutrient limitation in the ocean, *Nature*,  
498 339, 460-463, <http://doi.org/10.1038/339460a0>, 1989.
- 499 Foltz, G. R., and McPhaden, M. J.: Trends in Saharan dust and tropical Atlantic climate during  
500 1980 – 2006, *Geophys. Res. Lett.*, 35, L20706, <http://doi.org/10.1029/2008GL035042>, 2008.
- 501 Fowler, D., Pyle, J. A., Raven, J. A., and Sutton, M. A.: The global nitrogen cycle in the twenty-  
502 first century, *Philos. Trans. R. Soc. Lond. B Biol. Sci.*, 368, 1-13,  
503 <http://doi.org/10.1098/rstb.2013.0164>, 2013.
- 504 Galloway, J. N., Howarth, R. W., Michaels, A. F., Nixon, S. W., Prospero, J. M., and Dentener,  
505 F. J.: Nitrogen and phosphorus budgets of the North Atlantic Ocean and its watershed,  
506 *Biogeochemistry*, 35, 3-25, <http://doi.org/10.1007/BF02179823>, 1996.
- 507 Gruber, N.: The Marine Nitrogen Cycle, Overview and Challenges, in: *Nitrogen in the Marine*  
508 *Environment (2nd Edition)*, edited by: D. G. Capone, D. A. Bronk, M. R. Mulholland and E.  
509 J. Carpenter, Academic Press, San Diego, 1-50, [https://doi.org/10.1016/B978-0-12-372522-](https://doi.org/10.1016/B978-0-12-372522-6.00001-3)  
510 [6.00001-3](https://doi.org/10.1016/B978-0-12-372522-6.00001-3), 2008.
- 511 Gruber, N., and Deutsch, C. A.: Redfield's evolving legacy, *Nat. Geosci.*, 7, 853-855,  
512 <http://doi.org/10.1038/ngeo2308>, 2014.



- 513 Gruber, N., and Sarmiento, J.: Global patterns of marine nitrogen fixation and denitrification,  
514 *Global Biogeochem. Cycles*, 11, 235-266, <http://doi.org/10.1029/97GB00077>, 1997.
- 515 Hansell, D. A., Bates, N. R., and Olson, D. B.: Excess nitrate and nitrogen fixation in the North  
516 Atlantic Ocean, *Mar. Chem.*, 84, 243-265, <http://doi.org/10.1016/j.marchem.2003.08.004>,  
517 2004.
- 518 Hansell, D. A., Olson, D. B., Dentener, F., and Zamora, L. M.: Assessment of excess nitrate  
519 development in the subtropical North Atlantic, *Mar. Chem.*, 106, 562-579,  
520 <http://doi.org/10.1016/j.marchem.2007.06.005>, 2007.
- 521 Hastings, M. G., Sigman, D. M., and Lipschultz, F.: Isotopic evidence for source changes of  
522 nitrate in rain at Bermuda, *J. Geophys. Res. - Atmos.*, 108, 4790,  
523 <http://doi.org/10.1029/2003JD003789>, 2003.
- 524 Hydes, D., Aoyama, M., Aminot, A., Bakker, K., Becker, S., Coverly, S., Daniel, A., Dickson,  
525 A., Grosso, O., Kerouel, R., van Ooijen, J., Sato, K., Tanhua, T., Woodward, M., and Zhang,  
526 J.: Determination of dissolved nutrients (N, P, Si) in seawater with high precision and inter-  
527 comparability using gas-segmented continuous flow analysers, in: *The GO-SHIP Repeat*  
528 *Hydrography Manual: A Collection of Expert Reports and guidelines*. IOCCP Report No 14,  
529 ICPO Publication Series No. 134, version 1, UNESCO/IOC., 87, 2010.
- 530 Jickells, T., and Moore, C. M.: The importance of atmospheric deposition for ocean productivity,  
531 *Annu. Rev. Ecol. Evol. Syst.*, 46, 481-501, [http://doi.org/10.1146/annurev-ecolsys-112414-](http://doi.org/10.1146/annurev-ecolsys-112414-054118)  
532 054118, 2015.
- 533 Jickells, T. D., Buitenhuis, E., Altieri, K., Baker, A. R., Capone, D., Duce, R. A., Dentener, F.,  
534 Fennel, K., Kanakidou, M., LaRoche, J., Lee, K., Liss, P., Middelburg, J. J., Moore, J. K.,  
535 Okin, G., Oschlies, A., Sarin, M., Seitzinger, S., Sharples, J., Singh, A., Suntharalingam, P.,  
536 Uematsu, M., and Zamora, L. M.: A reevaluation of the magnitude and impacts of  
537 anthropogenic atmospheric nitrogen inputs on the ocean, *Global Biogeochem. Cycles*, 31,  
538 289-305, <http://doi.org/10.1002/2016GB005586>, 2017.
- 539 Kähler, P., Oschlies, A., Dietze, H., and Koeve, W.: Oxygen, carbon, and nutrients in the  
540 oligotrophic eastern subtropical North Atlantic, *Biogeosciences*, 7, 1143-1156,  
541 <http://doi.org/10.5194/bg-7-1143-2010>, 2010.
- 542 Key, R. M., Olsen, A., van Heuven, S., Lauvset, S. K., Velo, A., Lin, X., Schirnack, C., Kozyr,  
543 A., Tanhua, T., Hoppema, M., Jutterström, S., Steinfeldt, R., Jeansson, E., Ishii, M., Perez, F.





- 544 F., and Suzuki, T.: Global Ocean Data Analysis Project, Version 2 (GLODAPv2),  
545 (ORNL/CDIAC-162, ND-P093), Carbon Dioxide Information Analysis Center, Oak Ridge  
546 National Laboratory, US Department of Energy, 2015.
- 547 Kim, I.-N., Lee, K., Gruber, N., Karl, D. M., Bullister, J. L., Yang, S., and Kim, T.-W.:  
548 Increasing anthropogenic nitrogen in the North Pacific Ocean, *Science*, 346, 1102-1106,  
549 <http://doi.org/10.1126/science.1258396>, 2014a.
- 550 Kim, T.-W., Lee, K., Najjar, R. G., Jeong, H. D., and Jeon, H. J.: Increasing N abundance in the  
551 northwestern Pacific Ocean due to atmospheric nitrogen deposition, *Science*, 334, 505-509,  
552 <http://doi.org/10.1126/science.1206583>, 2011.
- 553 Kim, T.-W., Lee, K. Duce, R. and Liss, P.: Impact of atmospheric nitrogen deposition on  
554 phytoplankton productivity in the South China Sea, *Geophys. Res. Lett.*, 41,  
555 <http://doi.org/10.1002/2014GL059665>, 2014b.
- 556 Knapp, A. N., Hastings, M. G., Sigman, D. M., Lipschultz, F., and Galloway, J. N.: The flux and  
557 isotopic composition of reduced and total nitrogen in Bermuda rain, *Mar. Chem.*, 120, 83-89,  
558 <http://doi.org/10.1016/j.marchem.2008.08.007>, 2010.
- 559 Ko, Y. H., Lee, K., Takahashi, T., Karl, D. M., Kang, S.-H., and Lee, E.: Carbon-based estimate  
560 of nitrogen-fixation-derived net community production in N-depleted ocean gyres, *Global*  
561 *Biogeochem. Cycles*, 32, 1241-1252, <http://doi.org/10.1029/2017GB005634>, 2018.
- 562 Landolfi, A., Oschlies, A., and Sanders, R.: Organic nutrients and excess nitrogen in the North  
563 Atlantic subtropical gyre, *Biogeosciences*, 5, 1199-1213, [http://doi.org/10.5194/bg-5-1199-](http://doi.org/10.5194/bg-5-1199-2008)  
564 2008, 2008.
- 565 Lee, K.: Global net community production estimated from the annual cycle of surface water total  
566 dissolved inorganic carbon, *Limnol. Oceanogr.*, 46, 1287-1297,  
567 <http://doi.org/10.4319/lo.2001.46.6.1287>, 2001.
- 568 Lee, K., Karl, D. M., Wanninkhof, R., and Zhang, J.-Z.: Global estimates of net carbon  
569 production in the nitrate-depleted tropical and subtropical oceans, *Geophys. Res. Lett.*, 29,  
570 1907, <http://doi.org/10.1029/2001GL014198>, 2002.
- 571 Liu, X. Zhang, Y., Han, W., Tang, A., Shen, J., Cui, Z., Vitousek, P., Erisman, J. W., Goulding,  
572 K., Christie, P., Fangmeier, A., and Zhang, F.: Enhanced nitrogen deposition over China,  
573 *Nature*, 494, 459, <http://doi.org/10.1038/nature11917>, 2013.



- 574 Lomas, M. W., Burke, A. L., Lomas, D. A., Bell, D. W., Shen, C., Dyrhman, S. T., and  
575 Ammerman, J. W.: Sargasso Sea phosphorus biogeochemistry: an important role for dissolved  
576 organic phosphorus (DOP), *Biogeosciences*, 7, 695-710, [http://doi.org/10.5194/bg-7-695-](http://doi.org/10.5194/bg-7-695-2010)  
577 2010, 2010.
- 578 Luo, Y. W., Doney, S. C., Anderson, L. A., Benavides, M., Berman-Frank, I., Bode, A., Bonnet,  
579 S., Boström, K. H., Böttjer, D., Capone, D. G., Carpenter, E. J., Chen, Y. L., Church, M. J.,  
580 Dore, J. E., Falcón, L. I., Fernández, A., Foster, R. A., Furuya, K., Gómez, F., Gundersen, K.,  
581 Hynes, A. M., Karl, D. M., Kitajima, S., Langlois, R. J., LaRoche, J., Letelier, R. M.,  
582 Marañoñ, E., McGillicuddy Jr, D. J., Moisander, P. H., Moore, C. M., Mouriño-Carballido,  
583 B., Mulholland, M. R., Needoba, J. A., Orcutt, K. M., Poulton, A. J., Rahav, E., Raimbault,  
584 P., Rees, A. P., Riemann, L., Shiozaki, T., Subramaniam, A., Tyrrell, T., Turk-Kubo, K. A.,  
585 Varela, M., Villareal, T. A., Webb, E. A., White, A. E., Wu, J., and Zehr, J. P.: Database of  
586 diazotrophs in global ocean, abundance, biomass and nitrogen fixation rates, *Earth Syst. Sci.*  
587 *Data*, 4, 47-73, <http://doi.org/10.5194/essd-4-47-2012>, 2012.
- 588 Mahaffey, C., Michaels, A. F., and Capone, D. G.: The conundrum of marine N<sub>2</sub> fixation.  
589 *American J. Sci.* 305, 546-595. <http://doi.org/10.2475/ajs.305.6-8.546>, 2005.
- 590 Marconi, D., Sigman, D. M., Casciotti, K. L., Campbell, E. C., Alexandra Weigand, M., Fawcett,  
591 S. E., Knapp, A. N., Rafter, P. A., Ward, B. B., and Haug, G. H.: Tropical Dominance of N<sub>2</sub>  
592 Fixation in the North Atlantic Ocean, *Global Biogeochem. Cycles*, 31, 1608-1623,  
593 <http://doi.org/10.1002/2016GB005613>, 2017.
- 594 Mills, M. M., Ridame, C., Davey, M., La Roche, J., and Geider, R. J.: Iron and phosphorus co-  
595 limit nitrogen fixation in the eastern tropical North Atlantic, *Nature*, 429, 292-294,  
596 <http://doi.org/10.1038/nature02550>, 2004.
- 597 Moon, J.-Y., Lee, K., Tanhua, T., Kress, N., and Kim, I.-N.: Temporal nutrient dynamics in the  
598 Mediterranean Sea in response to anthropogenic inputs, *Geophys. Res. Lett.*, 43, 5243-5251,  
599 <http://doi.org/10.1002/2016GL068788>, 2016.
- 600 Moore, C. M.: Diagnosing oceanic nutrient deficiency, *Philos. Trans. Royal Soc. A*, 374,  
601 20150290, <http://doi.org/10.1098/rsta.2015.0290>, 2016.
- 602 Moore, C. M., Mills, M. M., Achterberg, E. P., Geider, R. J., LaRoche, J., Lucas, M. I.,  
603 McDonagh, E. L., Pan, X., Poulton, A. J., Rijkenberg, M. J. A., Suggett, D. J., Ussher, S. J.,



- 604 and Woodward, E. M. S.: Large-scale distribution of Atlantic nitrogen fixation controlled by  
605 iron availability, *Nat. Geosci.*, 2, 867-871, <http://doi.org/10.1038/ngeo667>, 2009.
- 606 Moore, C. M., Mills, M. M., Arrigo, K. R., Berman-Frank, I., Bopp, L., Boyd, P. W., Galbraith,  
607 E. D., Geider, R. J., Guieu, C., Jaccard, S. L., Jickells, T. D., La Roche, J., Lenton, T. M.,  
608 Mahowald, N. M., Marañón, E., Marinov, I., Moore, J. K., Nakatsuka, T., Oeschies, A., Saito,  
609 M. A., Thingstad, T. F., Tsude, A., and Ulloa, O.: Processes and patterns of oceanic nutrient  
610 limitation, *Nat. Geosci.*, 6, 701-710, <http://doi.org/10.1038/ngeo1765>, 2013.
- 611 Okin, G. S., Baker, A. R., Tegen, I., Mahowald, N. M., Dentener, F. J., Duce, R. A., Galloway, J.  
612 N., Hunter, K., Kanakidou, M., Kubilay, N., Prospero, J. M., Sarin, M., Surapipith, V.,  
613 Uematsu, M., and Zhu, T.: Impacts of atmospheric nutrient deposition on marine productivity,  
614 Roles of nitrogen, phosphorus, and iron, *Global Biogeochem. Cycles*, 25, GB2022,  
615 <http://doi.org/10.1029/2010GB003858>, 2011.
- 616 Olsen, A., Key, R. M., van Heuven, S., Lauvset, S. K., Velo, A., Lin, X., Schirnick, C., Kozyr,  
617 A., Tanhua, T., Hoppema, M., Jutterström, S., Steinfeldt, R., Jeansson, E., Ishii, M., Pérez, F.  
618 F., and Suzuki, T.: The Global Ocean Data Analysis Project version 2 (GLODAPv2) – an  
619 internally consistent data product for the world ocean, *Earth Syst. Sci. Data*, 8, 297-323,  
620 <http://doi.org/10.5194/essd-8-297-2016>, 2016.
- 621 Palter, J. B., Lozier, M. S., and Barber, R. T.: The effect of advection on the nutrient reservoir in  
622 the North Atlantic subtropical gyre, *Nature*, 437, 687-692,  
623 <http://doi.org/10.1038/nature03969>, 2005.
- 624 Palter, J. B., Lozier, M. S., Samiento, J. L., and Williams, R. G.: The supply of excess phosphate  
625 across the Gulf Stream and the maintenance of subtropical nitrogen fixation, *Global*  
626 *Biogeochem. Cycles*, 25, GB4007, <http://doi.org/10.1029/2010GB003955>, 2011.
- 627 Pelegrí, J. L., and Csanady, G. T.: Nutrient transport and mixing in the Gulf Stream, *J. Geophys.*  
628 *Res. – Oceans*, 96, 2577-2583, <http://doi.org/10.1029/90JC02535>, 1991.
- 629 Ren, H., Chen, Y.-C., Wang, X. T., Wong, G. T. F., Cohen, A. L., DeCarlo, T. M., Weigand, M.  
630 A., Mii, H.-S., and Sigman, D. M.: 21<sup>st</sup>-century rise in anthropogenic nitrogen deposition on a  
631 remote coral reef, *Science*, 356, 749-752, <http://doi.org/10.1126/science.aal3869>, 2017.
- 632 Ridley, D. A., Heald, C. L., and Prospero, J. M.: What controls the recent changes in African  
633 mineral dust aerosol across the Atlantic?, *Atmos. Chem. Phys.*, 14, 5735-5747,  
634 <http://doi.org/10.5194/acp-14-5735-2014>, 2014.



- 635 Ríos, A. F., Resplandy, L., García-Ibáñez, M. I., Fajar, N. M., Velo, A., Padin, X. A.,  
636 Wanninkhof, R., Steinfeldt, R., Rosón, G., and Pérez, F. F.: Decadal acidification in the water  
637 masses of the Atlantic Ocean, *Proc. Natl. Acad. Sci.*, 112, 9950-9955,  
638 <http://doi.org/10.1073/pnas.1504613112>, 2015.
- 639 Robson, J., Ortega, P., and Sutton, R.: A reversal of climatic trends in the North Atlantic since  
640 2005, *Nat. Geosci.*, 9, 513-517, <http://doi.org/10.1038/ngeo2727>, 2016.
- 641 Schmittner, A.: Decline of the marine ecosystem caused by a reduction in the Atlantic  
642 overturning circulation, *Nature*, 434, 628-633, <http://doi.org/10.1038/nature03476>, 2005.
- 643 Singh, A., Lomas, M. W., and Bates, N. R.: Revisiting N<sub>2</sub> fixation in the North Atlantic Ocean:  
644 Significance of deviations from the Redfield Ratio, atmospheric deposition and climate  
645 variability, *Deep Sea Res. Part II*, 93, 148-158, <http://doi.org/10.1016/j.dsr2.2013.04.008>,  
646 2013.
- 647 Singh, A., Baer, S. E., Riebesell, U., Martiny, A. C., and Lomas, M. W.: C, N, P stoichiometry  
648 at the Bermuda Atlantic Time-series Study station in the North Atlantic Ocean,  
649 *Biogeosciences*, 12, 6389-6403, <http://doi.org/10.5194/bg-12-6389-2015>, 2015.
- 650 Srokosz, M. A., and Bryden, H. L.: Observing the Atlantic Meridional Overturning Circulation  
651 yields a decade of inevitable surprises, *Science*, 348, <http://doi.org/10.1126/science.1255575>,  
652 2015.
- 653 St-Laurent, P., Friedrichs, M. A. M., Najjar, R. G., Martins, D. K., Herrmann, M., Miller, S. K.,  
654 and Wilkin, J.: Impacts of atmospheric nitrogen deposition on surface waters of the western  
655 North Atlantic mitigated by multiple feedbacks, *J. Geophys. Res. – Oceans*, 122, 8406-8426,  
656 <http://doi.org/10.1002/2017JC013072>, 2017.
- 657 Takahashi, T., Broecker, W. S., and Langer, S.: Redfield ratio based on chemical data from  
658 isopycnal surfaces, *J. Geophys. Res.*, 90, 6907-6924,  
659 <http://doi.org/10.1029/JC090iC04p06907>, 1985.
- 660 Vet, R., Artz, R. S., Carou, S., Shaw, M., Ro, C.-U., Aas, W., Baker, A., Bowersox, V. C.,  
661 Dentener, F., Galy-Lacaux, C., Hou, A., Pienaar, J. J., Gillett, R., Forti, M. C., Gromov, S.,  
662 Hara, H., Khodzher, T., Mahowald, N. M., Nickovic, S., Rao, P. S. P., and Reid, N. W.: A  
663 global assessment of precipitation chemistry and deposition of sulfur, nitrogen, sea salt, base  
664 cations, organic acids, acidity and pH, and phosphorus, *Atmos. Environ.*, 93, 3-100,  
665 <http://doi.org/10.1016/j.atmosenv.2013.10.060>, 2014.



- 666 Wang, X. T., Cohen, A. L., Luu, V., Ren, H., Su, Z., Haug, G. H., and Sigman, D. M.: Natural  
667 forcing of the North Atlantic nitrogen cycle in the Anthropocene, *Proc. Natl. Acad. Sci.*, 115,  
668 10606-10611, <http://doi.org/10.1073/pnas.1801049115>, 2018.
- 669 Williams, R. G., Roussenov, V., and Follows, M. J.: Nutrient streams and their induction into the  
670 mixed layer, *Global Biogeochem. Cycles*, 20, GB1016,  
671 <http://doi.org/10.1029/2005GB002586>, 2006.
- 672 Woosley, R. J., Millero, F. J., and Wanninkhof, R.: Rapid anthropogenic changes in CO<sub>2</sub> and pH  
673 in the Atlantic Ocean: 2003–2014, *Global Biogeochem. Cycles*, 30, 70-90,  
674 <http://doi.org/10.1002/2015GB005248>, 2016.
- 675 Yang, J. Y. T., Hsu, S. C., Dai, M. H., Hsiao, S. S. Y., and Kao, S. J.: Isotopic composition of  
676 water-soluble nitrate in bulk atmospheric deposition at Dongsha Island, sources and  
677 implications of external N supply to the northern South China Sea, *Biogeosciences* 11, 1833-  
678 1846, <http://doi.org/10.5194/bg-11-1833-2014>, 2014.
- 679 Yang, S., and Gruber, N.: The anthropogenic perturbation of the marine nitrogen cycle by  
680 atmospheric deposition, Nitrogen cycle feedbacks and the <sup>15</sup>N Habor-Bosch effect, *Global*  
681 *Biogeochem. Cycles*, 30, 1418-1440, <http://doi.org/10.1002/2016GB005421>, 2016.
- 682 Zamora, L. M., Landolfi, A., Oschlies, A., Hansell, D. A., Dietze, H., and Dentener F.:  
683 Atmospheric deposition of nutrients and excess N formation in the North Atlantic,  
684 *Biogeosciences*, 7, 777-793, <http://doi.org/10.5194/bg-7-777-2010>, 2010.
- 685 Zhang, J.-Z., Mordy, C. W., Gordon, L. I., Ross, A., and Garcia, H. E.: Temporal trends in deep  
686 ocean Redfield ratios, *Science*, 289, 1839-1839,  
687 <http://doi.org/10.1126/science.289.5486.1839a>, 2000.
- 688 Zhang, J.-Z., Wanninkhof, R., and Lee, K.: Enhanced new production observed from the diurnal  
689 cycle of nitrate in an oligotrophic anticyclonic eddy, *Geophys. Res. Lett.*, 28, 1579-1582,  
690 <http://doi.org/10.1029/2000GL012065>, 2001.



691 **Figure captions**

692 **Figure 1.** (a) Nutrient sampling locations (black dots) in the North Atlantic Ocean (NAtl).

693 All datasets from the meridional (A22, A20 and A16N) and zonal (A05) cruises were  
694 collected in the GLODAPv2 product and CLIVAR database (see text). The red dashed line  
695 indicates the region of STMW formation, and the solid arrows indicates streamlines of high  
696 transport in the western NAtl (i.e., the Gulf Stream, modified from Palter et al., 2005). The  
697 color scale indicates the model-derived atmospheric NO<sub>x</sub> deposition into the NAtl for 2000  
698 (Dentener et al., 2006).

699 **Figure 2.** The vertical distributions of DIN<sub>xs</sub> in the upper 1500 m for difference cruises along  
700 three meridional transects are shown in, (a) A22, (b) A20, and (c) A16N, respectively. The  
701 insets in (a–c) show the average rates (with 95% confidence limits) of  $\Delta$ DIN<sub>xs</sub> at 200–600 m  
702 and 1200–1500 m averaged for each 3°–8° latitude interval between GO-SHIP (2010s) and  
703 WOCE (late 1980s to 1990s) time periods along each transect (see Table S1).

704 **Figure 3.** Temporal trends of DIN<sub>xs</sub> anomalies (dots) for the corresponding latitude interval  
705 for the subsurface potential density intervals  $\sigma_\theta$  along the three meridional transects (a) A22,  
706 (b) A20, and (c) A16N in the NAtl. Data from A05 obtained in 2010 at three crossover sites  
707 are also shown (triangles). mDIN<sub>xs</sub> values in parentheses indicate the mean DIN<sub>xs</sub> in GO-  
708 SHIP dataset. The selected  $\sigma_\theta$  intervals are typically located at the depth intervals of 200–600  
709 m with DIN<sub>xs</sub> maximum along each transect. Note that the selected  $\sigma_\theta$  interval (= 27.2–27.6)  
710 in the subpolar region along A16N (45°N–60°N) is different from that in the subtropical  
711 region, as  $\sigma_\theta$  for 200–600 m depth becomes larger in the high-latitude region. Besides repeat  
712 cruises of these transects, the data sets from other cruises with similar tracks (Fig. 1) in the  
713 sub-regions were included for comparison. The DIN<sub>xs</sub> values were corrected by the changes  
714 in AOU to remove the contribution from remineralization of organic matter (see text). The  
715 data points connected by the dashed lines indicate that the  $\Delta$ DIN<sub>xs</sub> were statistically



716 significant in these regions ( $p < 0.05$ , Student's t-test and ANOVA with Games-Howell test).  
717 Otherwise, the data that were statistically unchanged are not connected by the dashed lines.  
718 The smoothed trend using the 5-year rLowess filter for  $\text{DIN}_{\text{xs}}$  anomalies of the STMW at the  
719 same depth ranges of the BATS site (near A22) is also shown (the gray shading in a). The  
720 gray dashed lines indicate  $\text{DIN}_{\text{xs}}$  anomaly equals to zero.

721 **Figure 4.** As for Figure 3, except for DIP anomalies. mDIP values in parentheses indicate the  
722 mean DIP in GO-SHIP dataset. The gray dashed lines indicate DIP anomaly equals to zero.  
723 Date from the BATS site are also included in (a).

724 **Figure 5.** (a) The rates of  $\Delta\text{DIN}_{\text{xs}}$  in the subsurface waters (200–600 m) along the four  
725 transects between GO-SHIP and WOCE time periods (see Table S1). The study area is  
726 divided into 10 subregions of  $10^\circ$  longitude by  $5^\circ$ – $15^\circ$  latitude along the transects A22  
727 (boxes 1–2), A20 (boxes 3–5), part of A05 (box 6) and A16N (boxes 7–10). The statistically  
728 significant changes (Student's t test and ANOVA with Games-Howell test,  $p < 0.05$ ) are  
729 marked with the superscript “t” for the box numbers. (b) Temporal variations of  $\text{DIN}_{\text{xs}}$   
730 anomalies (open dots and their fitting curve as black curve) in the western NATl in which the  
731 subsurface  $\text{DIN}_{\text{xs}}$  increased significantly (boxes 1–3 in a). Trend in  $\text{DIN}_{\text{xs}}$  anomalies in the  
732 subsurface waters at the BATS site is shown in gray shading (the same as Fig. 3a). To ensure  
733 consistent comparisons between atmospheric N deposition rates and seawater  $\text{DIN}_{\text{xs}}$   
734 anomalies, the seawater  $\text{DIN}_{\text{xs}}$  anomaly values were shifted by approximately 15 years. The  
735 15-year shift corresponded to the mean time period that had elapsed since a given subsurface  
736 water mass had last been in contact with the atmosphere prior to subduction. The year that the  
737 subsurface water mass in the NATl last had contacted the atmosphere was calculated using the  
738 CFCs contents in that subsurface water. The history of observed atmospheric wet deposition  
739 (WD) of  $\text{NO}_x$  from the US Atlantic coast. Orange curve and its shading show the 5-year  
740 moving average values and the range of the 95% confidence intervals, respectively (the

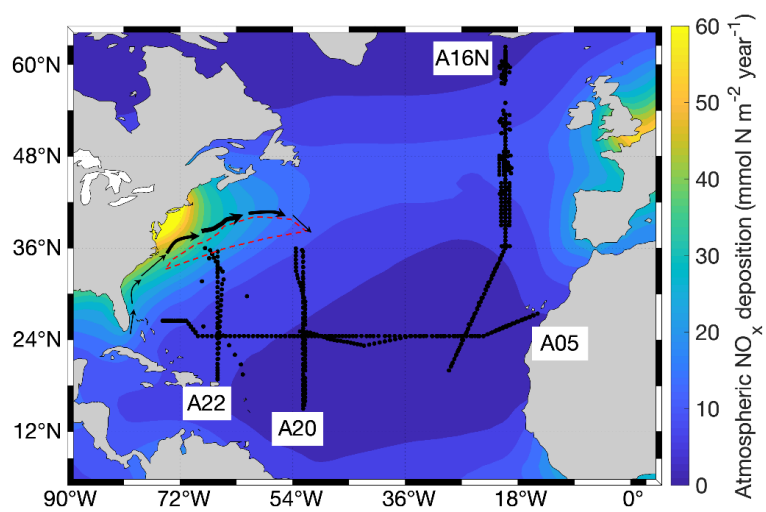


741 monitoring sites are presented in Table S3). Blue curve indicates the NO<sub>x</sub> emission from the  
742 USA. The NO<sub>x</sub> emission strongly correlates with the WD of NO<sub>x</sub> ( $r = 0.93$ ,  $p < 0.01$ ).



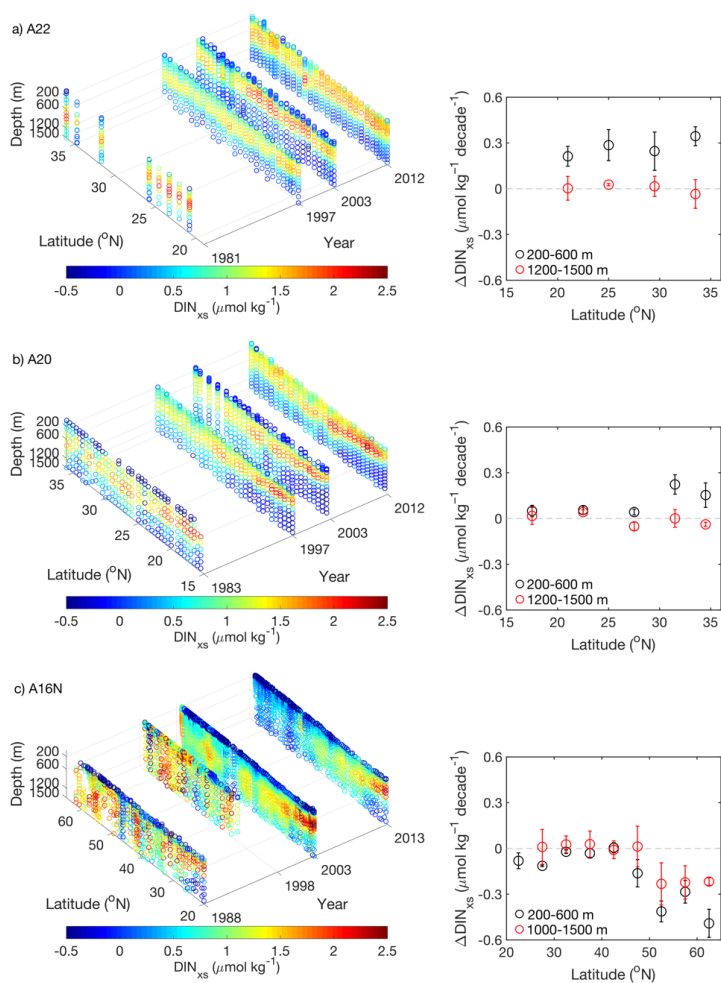


743 **Figure 1**





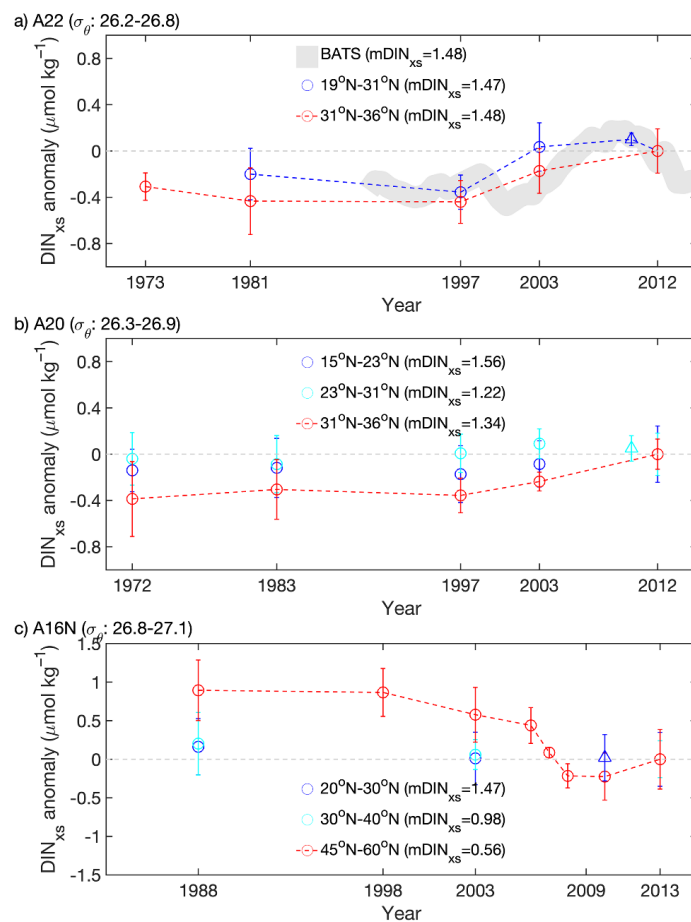
745 **Figure 2**



746



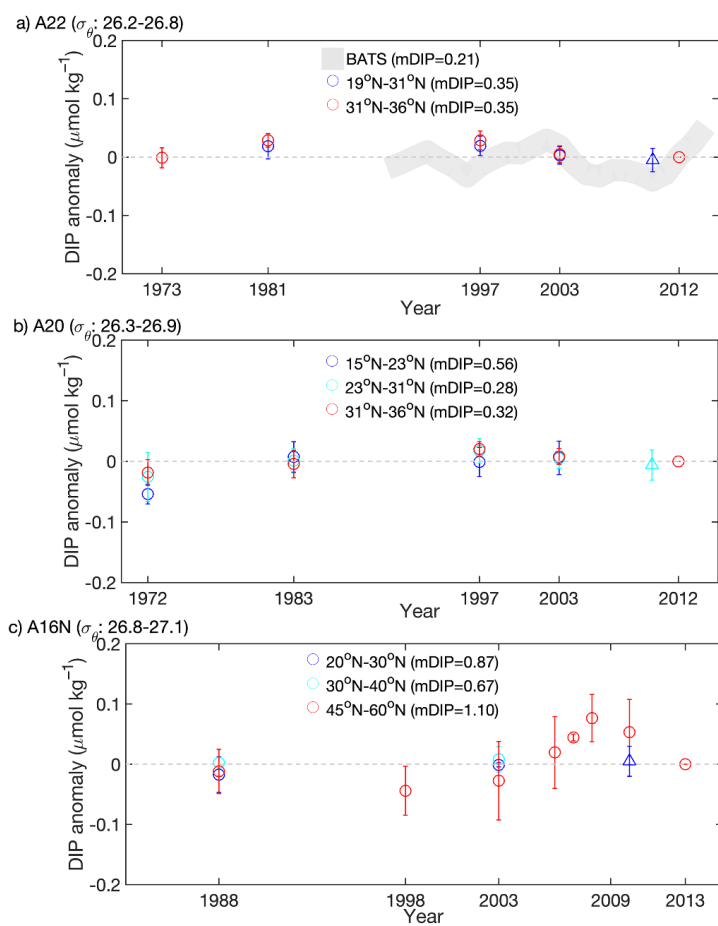
747 **Figure 3**



748



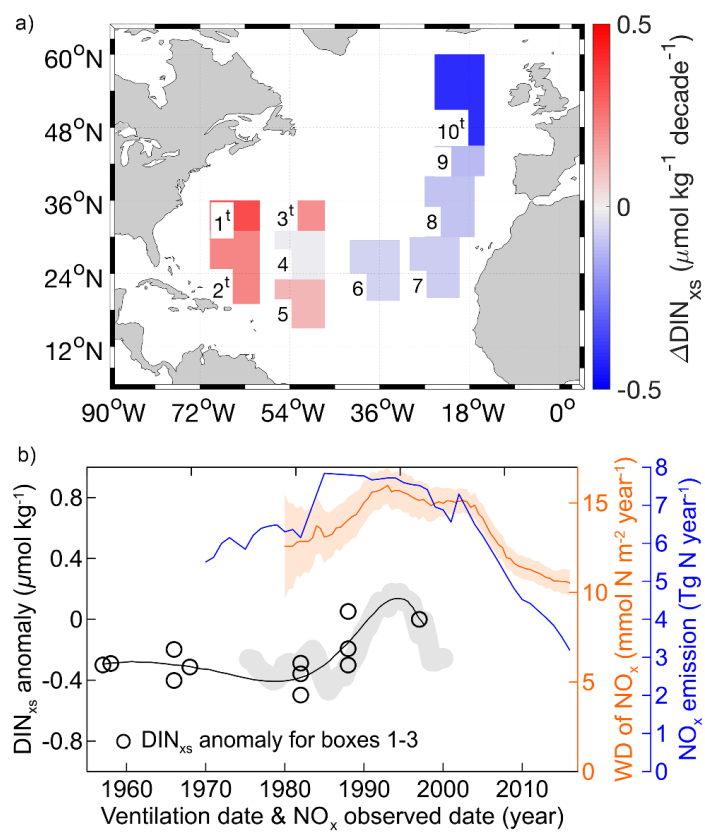
749 **Figure 4**



750



751 **Figure 5**



752

753